Use of stable isotopically labeled tracers to measure very low density lipoprotein-triglyceride turnover

Bruce W. Patterson,[1] Bettina Mittendorfer, Nizar Elias, Raj Satyanarayana, and Samuel Klein

Center for Human Nutrition, Department of Internal Medicine, Washington University School of Medicine, 660 South Euclid Avenue, Campus Box 8031, St. Louis, MO 63110

Abstract **Tracer methods for VLDL-TG kinetics vary in their ability to account for the effect of tracer recycling, which can influence the calculation of VLDL-TG fractional catabolic rates (FCRs). We evaluated a novel approach, involving stable isotopically labeled glycerol or palmitate tracers in conjunction with compartmental modeling, for measuring VLDL-TG kinetics in normolipidemic human subjects. When administered as a bolus simultaneously, both tracers provided identical VLDL-TG FCRs when the data were analyzed by a compartmental model that accounted for hepatic lipid tracer recycling, but not by non-compartmental analysis. The model-derived FCR was greater than that determined using a non-compartmental approach, and was 2- to 3-fold higher than that usually reported by using a bolus of radioactive [^{3}H]glycerol. When palmitate tracer was given as a constant infusion, VLDL-TG turnover appeared 5-fold slower, because tracer recycling through hepatic lipid pools could not be resolved with the infusion protocol. We conclude that accounting for tracer recycling, particularly the contribution of hepatic glycerolipid pools, is essential to accurately measure VLDL-TG kinetics, and that bolus injection of stable isotopically labeled glycerol or palmitate tracers in conjunction with compartmental modeling analysis offers a reliable approach for measuring VLDL-TG kinetics.**—Patterson, B. W., B. Mittendorfer, N. Elias, R. Satyanarayana, and S. Klein. **Use of stable isotopically labeled tracers to measure very low density lipoprotein-triglyceride turnover.** ***J. Lipid Res.*** **2002.** 43: **223–233.**

Supplementary key words compartmental modeling • non-compartmental modeling • tracer kinetics • tracer recycling • fractional catabolic rate • liver

TG synthesized in the liver is secreted into plasma as part of VLDL. The production of VLDL permits the delivery of hydrophobic triglyceride fuel from the liver to other tissues for energy metabolism. However, elevated plasma triglyceride concentration is associated with diabetes (1) and obesity (2) and is a risk factor for cardiovascular disease (3). Therefore, understanding VLDL-TG metabolism has important physiological and clinical implications.

Radioisotopically labeled tracers (^{3}H, ^{14}C) of glycerol or fatty acids are often used to study TG metabolic kinetics. One common approach is to inject a bolus of tracer and determine the subsequent monoexponential slope of the decline in plasma VLDL-TG specific radioactivity (4–7). However, this approach can underestimate the true VLDL-TG turnover rate because it does not account for tracer recycling. Compartmental modeling improves the accuracy of measuring VLDL-TG kinetics by bolus tracer injection, because the model attempts to account for tracer recycling (8–12). Glycerol is considered to be a better tracer than palmitate because glycerol recycles to a lesser extent than fatty acids (4). However, not all glycerol tracers are equivalent; [2-^{3}H]glycerol recycles less than [^{14}C]glycerol because the hydrogen on carbon 2 is lost when glycerol-3-phosphate is converted to dihydroxyacetone phosphate during glycolysis (8).

Whenever possible, stable isotope tracers, rather than radioactive tracers, should be used for research in human subjects because of the absence of radiation exposure with stable isotope tracers. Although stable isotopically labeled amino acid tracers have been used extensively to measure the metabolic kinetics of the protein moieties of plasma lipoproteins (13–19), the use of stable isotopically labeled tracers to evaluate plasma TG metabolism has been limited. Moreover, the current stable isotope approaches have methodological limitations that may decrease their reliability and usefulness in clinical studies. We recently found that VLDL-TG kinetics, determined by using the monoexponential slope technique, was 18% faster with [$^2H_5$]glycerol compared with [2-^{3}H]glycerol when the tracers were given as a simultaneous bolus, demonstrating that these two tracers may provide different estimates of VLDL-TG turnover rates (20). A constant infusion of stable isotopically labeled glycerol or palmitate has been used to measure VLDL-TG turnover rates by fitting the data to a monoexponential rise-to-plateau model (21–23). However, this method does not account for the con-

Abbreviations: FAME, fatty acid methyl ester; FCR, fractional catabolic rate; FSR, fractional synthetic rate; GC-MS, gas chromatography-mass spectrometry; HFB, heptafluorobutyrl; TTR, tracer-tracee ratio.

[1] To whom correspondence should be addressed.
e-mail: bpatters@im.wustl.edu

siderable tracer recycling that occurs during a prolonged constant infusion protocol. The rates of de novo lipogenesis, VLDL-TG fatty acids, and VLDL-TG fractional turnover has been evaluated by measuring the incorporation of [^{13}C]acetate combined in conjunction with mass isotopomer distribution analysis (24). Although this approach is valid, it is limited to conditions under which lipogenesis occurs and has limited utility under fasting conditions (20). The rate of appearance (Ra) of VLDL-TG has been measured by using a model-independent approach involving re-infusion of VLDL that has been pre-labeled with [^{13}C]glycerol (25). Unfortunately, this approach is difficult because it requires producing endogenously labeled VLDL-TG, plasmapheresis, and VLDL isolation and storage before re-infusion.

The purpose of the present study was to evaluate a novel approach for measuring VLDL-TG turnover by using stable isotopically labeled glycerol or palmitate tracers in conjunction with mathematical modeling. In theory, if the method is accurate, the use of labeled glycerol or palmitate tracers should yield the same value for VLDL-TG turnover. All aspects of the methodology are detailed, including choice of tracers, execution of clinical protocols, sample processing, analysis by gas chromatography-mass spectrometry (GC-MS), and determination of VLDL-TG turnover rates from the experimental data.

MATERIALS AND METHODS

Study subjects

A total of 44 subjects were studied. These subjects were participating in a series of studies designed to evaluate the regulation of VLDL-TG metabolism. At the same time, each study was also designed to evaluate tracer methods for assessing VLDL-TG kinetics to determine the most reliable approach. The present report will review the data validating our proposed method for determining VLDL-TG turnover rates; the assessment of factors that influence VLDL-TG turnover and production rates will be presented elsewhere.

Three groups of subjects participating in separate research protocols were studied. One group included eight lean [five male, three female, age 40.0 ± 3.0 years, body weight 71.9 ± 3.7 kg, body mass index (BMI) 23.7 ± 0.8 kg/m^2] and seven obese (four male, three female, age 38.4 ± 3.5 years, body weight 102.9 ± 5.4 kg, BMI 36.1 ± 1.2 kg/m^2) subjects. In these subjects, an intravenous bolus of glycerol and palmitate tracers was given during basal postabsorptive conditions and during intravenous infusion of glucose (5.5 mg/kg fat free mass/min, initiated 10 h before tracer administration and maintained throughout the study period). This study compared bolus glycerol with bolus palmitate tracer and the use of the monoexponential slope technique with compartmental modeling. A second group included five lean (one male, four female, age 25.4 ± 1.7 years, body weight 57.8 ± 3.3 kg, BMI 20.9 ± 0.3 kg/m^2) and fifteen obese (one male, fourteen female, age 37.9 ± 2.2 years, body weight 103.7 ± 3.0 kg, BMI 36.2 ± 0.8 kg/m^2) subjects. Five of the obese subjects were studied on a second occasion after losing 10% of their body weight. In these subjects, an intravenous bolus of glycerol tracer and a constant infusion of palmitate tracer were given during basal postabsorptive conditions. This study compared bolus glycerol tracer injection and compartmental modeling with the constant infusion of palmitate tracer and rise-to-plateau techniques. A third group included five lean subjects (three male, two female, age 28.2 ± 4.7 years, BMI 26.8 ± 2.6 kg/m^2) and four subjects with hypobetalipoproteinemia (two male, two female, age 33.3 ± 6.6 years, BMI 26.7 ± 1.6 kg/m^2) who received an intravenous bolus of glycerol tracer during basal postabsorptive conditions. The data from these subjects were previously reported as part of another study (19) and were included here in the comparison of the monoexponential slope analysis with compartmental modeling analysis after bolus injection of glycerol tracer.

All subjects completed a comprehensive medical evaluation, which included a history and physical examination, an electrocardiogram, and standard blood tests. All subjects had normal fasting triglyceride levels (<200 mg/dl). None of the subjects were taking regular medications or smoked tobacco, and all were weight stable for at least 4 weeks before the study. Written informed consent was obtained from all subjects before their participation in the study, which was approved by the Human Studies Committee and the General Clinical Research Center (GCRC) Scientific Advisory Committee of Washington University School of Medicine.

Experimental protocol

Subjects were admitted to the GCRC at Washington University School of Medicine in the evening before the isotope infusion study. At 1900 h, subjects consumed a standard meal containing 55% of total energy as carbohydrate, 30% as fat, and 15% as protein. At 2000 h, the subjects ingested a liquid formula (Ensure™, Ross Laboratories, Columbus, OH), containing 250 kcal (40 g carbohydrates, 6.1 g fat, and 8.8 g protein), and then fasted until completion of the study the next day.

The following morning, an isotope infusion study was performed to measure VLDL-TG kinetics. Subjects remained at rest in bed for the entire duration of the study. At 0530 h, catheters were inserted into a forearm vein for isotope infusion and into a contralateral hand vein, which was heated, for arterialized blood sampling. At 0700 h (time = 0), after a blood sample was obtained to determine background isotopic enrichments in plasma, a bolus of [1,1,2,3,3-^{2}H$_5$]glycerol (50–75 μmol/kg; Cambridge Isotope Laboratories, Andover, MA) dissolved in 0.9% saline was administered intravenously. In studies that included a bolus of labeled palmitate (6 μmol/kg of either [1-^{13}C]palmitate or [2,2-^{2}H$_2$]palmitate, Cambridge Isotope Laboratories, bound to human serum albumin), glycerol and palmitate tracers were mixed together and given simultaneously. In studies that included a constant infusion of labeled palmitate, the glycerol bolus was immediately followed by a 12 h constant infusion (0.035 μmol/kg/min) of [2,2-^{2}H$_2$]palmitate bound to serum albumin, that was given by using a syringe infusion pump (Harvard Bioscience Inc., Holliston, MA). Blood samples were obtained at 5, 15, 30, 45, and 60 min and then every hour for 12 h to determine plasma substrate concentrations and plasma glycerol and VLDL-TG tracer-to-tracee ratios (TTRs).

Blood samples were placed in chilled tubes containing EDTA and placed on ice. Plasma was recovered by low speed centrifugation within 30 min of sample collection. An aliquot of plasma (2 ml) was kept in the refrigerator for subsequent isolation of VLDL and the remaining plasma was frozen at −70°C for further processing.

Sample processing

VLDL was recovered by overlayering 2 ml plasma with a density 1.006 g/ml solution, followed by ultracentrifugation for 16 h at 45,000 rpm, 8°C, in a type 50.4 Ti rotor (Beckman Instruments, Palo Alto, CA). VLDL was recovered in the upper 1.5 ml

volume by tube slicing. VLDL apolipoprotein B-100 was precipitated by the method of Klein and Zilversmit (26). The aqueous and solvent extraction layers containing VLDL lipids and soluble apolipoproteins were combined, extracted with 1.5 ml of chloroform-methanol (3:1, v/v), and the bottom layer containing VLDL lipids was dried under vacuum (SpeedVac centrifugational concentrator, Savant, Farmingdale, NY). VLDL-TG were isolated by thin layer chromatography (TLC) on LK6D silica gel plates (Whatman, Clifton, NJ) using heptane-diethyl ether-formic acid (80:20:2, v/v/v) and visualized with 0.01% rhodamine 6G. TLC scrapings containing TGs were recovered, extracted with chloroform-methanol (3:1, v/v), transferred to 13 mm screw-top vials and dried under vacuum. Fatty acid methyl esters (FAMEs) were prepared by adding 0.5 ml of 10% acetyl chloride in methanol, capping the tubes with Teflon-lined caps, incubated at 70°C for 30 min, and dried under vacuum. The glycerol liberated by the transmethylation reaction was derivatized by the addition of 200 μl 5% heptafluorobutyric (HFB) anhydride in ethyl acetate. Capped vials were incubated at 70°C for 30 min. After drying under vacuum, 100 μl ethyl acetate was added and samples were transferred to autosampler vials for GC-MS analysis of HFB-glycerol and palmitate methyl ester in the same run.

Plasma glycerol and palmitate were recovered from 0.25 ml plasma after precipitation of plasma proteins with acetone and extraction of the aqueous phase with hexane (27). The aqueous phase containing glycerol was dried under vacuum (SpeedVac) and derivatized with 100 μl of HFB anhydride-ethyl acetate (1:1, v/v) at 70°C for 10 min. After drying in a SpeedVac, the samples were dissolved in 100 μl ethyl acetate.

Sample analyses

The isotopic enrichment of palmitate methyl ester and glycerol were measured by selected ion monitoring electron impact ionization GC-MS by using a HP5973 mass selective detector (Hewlett-Packard, Palo Alto, CA) equipped with a 30 m × 0.25 mm DB-17 capillary column (Supelco, Bellefonte, PA). The molecular ion of palmitate methyl ester was monitored at mass-to-charge-ratio (*m/z*) 270, 271, and 272, corresponding to the unlabeled, ^{13}C-, and $^{2}H_2$-labeled palmitate. Samples were adjusted to approximately constant concentrations to minimize artifacts due to concentration-dependent self-chemical ionization of methyl palmitate (27, 28). Ions of HFB-glycerol were monitored at *m/z* 467, 468, and 472 that corresponds to loss of *O*-HFB from the molecular ion (29) for unlabeled ^{13}C- and $^{2}H_5$-labeled glycerol. The VLDL-TG HFB-glycerol and palmitate methyl ester were monitored within the same GC-MS run. The TTR of glycerol and palmitate were determined by calibration against standards of known isotopic enrichment (30).

Kinetic analyses

Bolus injection of tracer. Kinetic parameters were independently determined for glycerol and palmitate tracers. Although both tracers were injected simultaneously, no constraints were applied to combine the two tracers into a single kinetic analysis. The monoexponential slopes of VLDL-TG glycerol and palmitate were determined from the peak of isotopic enrichment to the last point that, by visual inspection, fell on the log-linear portion of the curve (usually 6 h to 8 h) (5). In addition, compartmental modeling was used to provide a more comprehensive analysis of VLDL-TG tracer kinetics (**Fig. 1**) based on the model developed by Zech et al. (8) for VLDL-TG following a bolus of [2-^{3}H]glycerol. The time course of plasma glycerol or palmitate TTR was described as a "forcing function," defined as a linear interpolation between observed time points. This time course accounted for systemic recycling of glycerol and palmitate tracers between

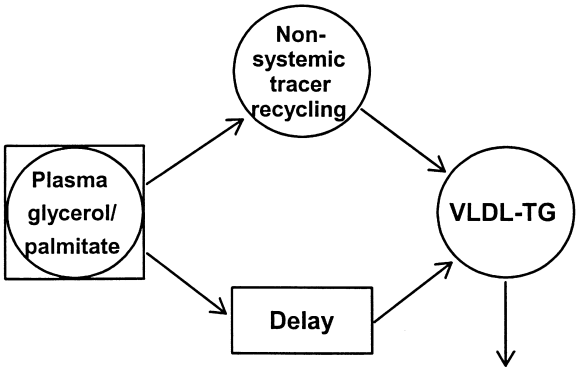

Fig. 1. Compartmental model for turnover kinetics of VLDL-TG by using stable isotopically labeled glycerol and palmitate. Glycerol or palmitate tracer is injected into plasma. A "fast" synthetic pathway comprises a short time delay for synthesis, assembly, and secretion of VLDL-TG, and a "slow" pathway accounts for non-systemic tracer recycling (tracer that is removed from plasma, placed into pools that turn over, and contribute tracer to VLDL-TG secretion after the bolus has cleared through the system). The primary kinetic parameter measured by this model is the fractional catabolic rate of VLDL-TG (loss of VLDL-TG tracer from the system).

plasma and peripheral tissues. As proposed by Zech et al. (8), there are two biosynthetic pathways between plasma glycerol or palmitate and VLDL-TG. The "fast" pathway comprises a time delay (typically 0.5 h) to account for TG synthesis, VLDL packaging, and secretion. A "slow" pathway represents a pool of tracer (presumably labeled hepatic glycerolipids) that turn over at a rate of approximately 0.3 pools/h (adjustable parameter), which provides a source of non-systemic tracer recycling. Inclusion of the "slow" pathway was necessary to fit the terminal tail of VLDL-TG enrichment when bolus tracers were used. A single compartment was adequate to describe VLDL-TG tracer kinetics, and VLDL-TG kinetic heterogeneity was not evident in any of our subjects. The fractional catabolic rate (FCR) of VLDL-TG was the fraction of the plasma VLDL-TG pool lost per h. Compartmental modeling was performed using the SAAM II program (SAAM Institute, University of Washington, Seattle).

A nonlinear function was used to describe the fraction of plasma glycerol or palmitate that is taken up by the VLDL-TG synthetic pathways because the bolus doses of palmitate and glycerol do not represent massless quantities of tracer. This function is calculated as:

$$k_t = k_0 / (1 + TTR_t)$$

where k_t is the fractional rate constant for a given time t (different values for the fast and slow pathways), k_0 is the fractional rate constant at the limit of zero enrichment, and TTR_t is the plasma tracer enrichment at time t. This nonlinear relationship ensures that the amount rather than fraction of plasma glycerol or palmitate used for VLDL-TG synthesis remains constant over time.

Constant infusion of tracer. The turnover rate of VLDL-TG following a constant infusion of labeled palmitate was determined by using the compartmental model shown in Fig. 1. In addition, two non-compartmental approaches were used to determine the VLDL-TG turnover rate for the infused palmitate tracer. First, the fractional synthetic rate (FSR) was determined by dividing the initial slope (usually between 0.5 h and 2.5 h) by the plateau enrichment (usually the average value between 10 h and 12 h if a plateau was apparent) (30). At metabolic steady state, VLDL-TG FSR should equal VLDL-TG FCR. Second, the entire VLDL-TG

palmitate time course was described by a monoexponential rise-to-plateau mathematical model (30):

$$TTR_t = TTR_p\ (1 - e^{-k(t-d)}),$$

where TTR_t is the enrichment at time t, TTR_p is the plateau enrichment, k is the rate constant for VLDL-TG turnover (pools h^{-1}), and d is a time delay. Least squares curve fitting was accomplished using the Solver function within Microsoft Excel (Microsoft, Seattle, WA).

Statistical analysis

A two-tailed students *t*-test for paired samples was performed to evaluate the statistical significance of the differences in values for VLDL-TG kinetics obtained from the use of different tracers and different mathematical models. Simple linear regression was used to determine the relationship between variables. A *P* value ≤ 0.05 was considered to be statistically significant. All statistical analyses were performed by using Microsoft Excel. Data are reported as means ± SEM.

RESULTS

Bolus glycerol and palmitate tracer injection

Glycerol and palmitate TTRs. Plasma glycerol TTR and palmitate TTR after bolus tracer injection in a representative subject is shown in **Fig. 2A**. Plasma glycerol and palmitate TTRs were maximal 5 min after injection (average values were 1.12 ± 0.20 and 0.40 ± 0.14, respectively), decreased by three orders of magnitude within 2–3 h, and were virtually undetectable after 4–6 h. Glycerol TTR and palmitate TTR in plasma VLDL-TG in a representative subject are shown in Fig. 2B. There was usually a 30-min delay before glycerol and palmitate TTR was detectable in VLDL-TG, which peaked at 1–2 h after bolus tracer injection.

The GC-MS and kinetic analyses of the glycerol tracer in VLDL-TG were based on measuring the TTR from the m+5/m+0 ratio of glycerol in VLDL-TG. However, we found evidence of extensive loss of deuterium from VLDL-TG glycerol, which presumably occurred during different stages of glycolysis, which resulted in m+4-, m+3-, m+2-, and m+1-labeled glycerol, representing a loss of 1–4 deuteriums from [$^2H_5$]glycerol (**Fig. 3**). Labeled glycerol isotopomers appeared parallel on a log plot (results not shown), suggesting they exhibited identical VLDL-TG kinetics. The prominence of m+1- and m+2-labeled glycerol in relation to the starting m+5 was variable, at times being greater than the m+5 (as shown in Fig. 3), whereas the m+5 predominated at other times. Loss of deuterium from free plasma [$^2H_5$]glycerol was not observed, nor was it observed for a [$^2H_5$]glycerol standard subjected to treatment with acetyl chloride and methanol as in VLDL-TG processing (data not shown).

Monoexponential slope. A monoexponential slope of the decline in VLDL-TG TTR could be reliably determined over a 3–6 h period following peak enrichment (Fig. 2C).

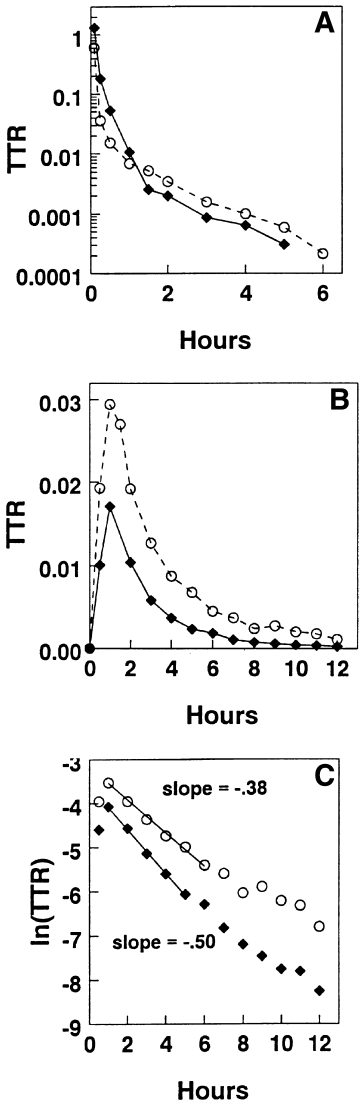

Fig. 2. Plasma [$^2H_5$]glycerol (solid diamonds) and [^{13}C]palmitate (open circles) tracer-tracee ratios (TTRs) in plasma (A), in VLDL-TG (B), and in VLDL-TG in conjunction with a monoexponential slope analysis (C) in a representative subject.

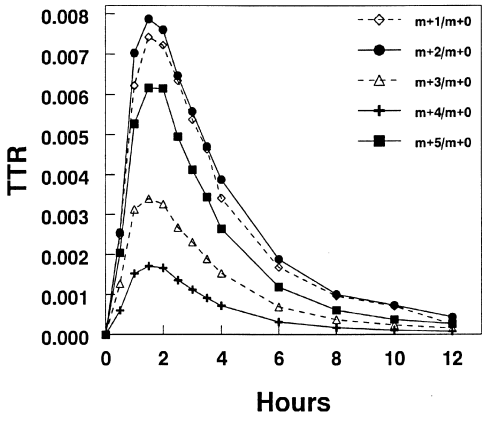

Fig. 3. Loss of deuterium from [$^2H_5$]glycerol tracer incorporated into VLDL-TG. The isotopic enrichment of all isotopomers of labeled glycerol in VLDL-TG was measured after a bolus tracer of [$^2H_5$]glycerol was administered. Points represent the average of triplicate measurements for a representative subject.

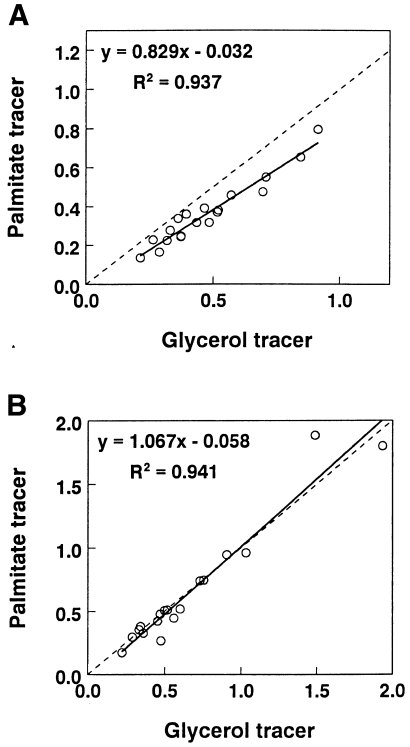

Fig. 4. Comparison of VLDL-TG turnover rates using simultaneous bolus injections of [$^2H_5$]glycerol with either [$^2H_2$]- or [^{13}C]palmitate. Turnover rates (pools/h) for VLDL-TG turnover were independently determined for both tracers. Dashed lines represent lines of identity. A: Kinetic analysis performed by monoexponential slope from peak VLDL-TG isotopic enrichment for both glycerol and palmitate tracers. B: Kinetic analysis performed by the compartmental model shown in Fig. 1 that accounts for non-systemic tracer recycling. Same studies as shown in A.

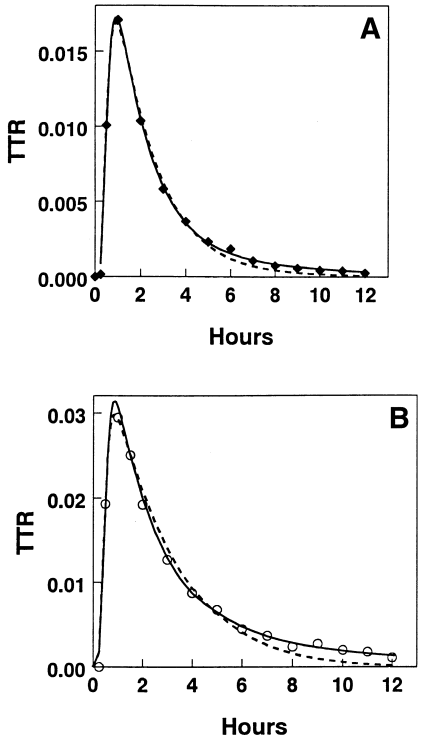

Fig. 5. VLDL-TG enrichment described by compartmental modeling. The VLDL-TG enrichment for [$^2H_5$]glycerol (A) and [^{13}C]palmitate (B) were fit to the compartmental model shown in Fig. 1. Same subject as illustrated in Fig. 2. Two fits are shown for each tracer. Dashed line, shows fit to the model with the "slow" production pathway omitted. Solid line, shows fit to the model with the "slow" production pathway included.

The slopes of the VLDL-TG glycerol and palmitate TTRs diminished beyond this period because of tracer recycling. Although there was a good correlation (R^2 = 0.93) between apparent turnover rates determined by the glycerol and palmitate tracers using the monoexponential slope analysis, the palmitate tracer systematically produced lower apparent VLDL-TG turnover rates than the glycerol tracer (slope = 0.83 ± 0.05, intercept not significantly different from zero, **Fig. 4A**). For example, the apparent VLDL-TG turnover rate determined by the monoexponential slope for the subject illustrated in Fig. 2 was 0.38 h^{-1} with the palmitate bolus and 0.50 h^{-1} with the glycerol bolus.

Compartmental model. The compartmental model shown in Fig. 1 provided an excellent fit to all sets of VLDL-TG glycerol and palmitate tracer data. The representative example shown in **Fig. 5** involves the data from the subject shown in Fig. 2. When the "slow" production pathway was omitted from the model, the model systematically overestimated the data for the middle portion of the descending curve (2–3 h for the data set illustrated) and underestimated the data for the terminal portion of the curve (Fig. 5, dashed lines). The systematic errors in describing the shape of the VLDL-TG peaks when the "slow" production pathway was omitted caused us to reject this variation of the model.

When the "slow" pathway was incorporated into the model to account for non-systemic tracer recycling, nearly perfect fits to the data were obtained (Fig. 5, solid lines) without evidence of systematic deviations. Inclusion of the "slow" pathway reduced the sum-of-squares to the same extent (approximately 50%) for both the glycerol and palmitate tracers. There was excellent agreement between data derived from the glycerol and palmitate tracers when the VLDL-TG turnover rate was determined by using the compartmental model. For example, in the study illustrated in Fig. 5, VLDL-TG FCR was 0.73 and 0.74 h^{-1} with glycerol and palmitate tracers, respectively. Regression analysis resulted in a line not significantly different from a line of identity (slope = 1.06 ± 0.06, intercept not significantly different from zero, R^2 = 0.94; Fig. 4B).

The relationship between the VLDL-TG FCR determined by the compartmental model and the monoexponential slope was curvilinear when either glycerol or palmitate tracer was used (**Fig. 6**). With use of the glycerol tracer, the two kinetic analyses provided similar values when the turnover rate was sufficiently slow (<0.5 h^{-1}), but the model-derived FCR rapidly increased in relation to the monoexponential slope when the turnover rate was greater than 0.5 h^{-1} (Fig. 6A). With use of the palmitate

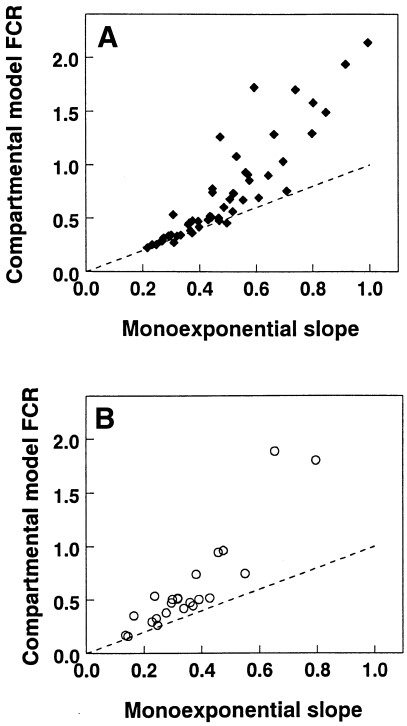

Fig. 6. Correlation between the compartmental model-derived VLDL-TG FCR and the apparent VLDL-TG turnover rate by the monoexponential slope approach. Rate constants are as pools/h. Dashed lines represent lines of identity. A: Glycerol tracer. B: Palmitate tracer.

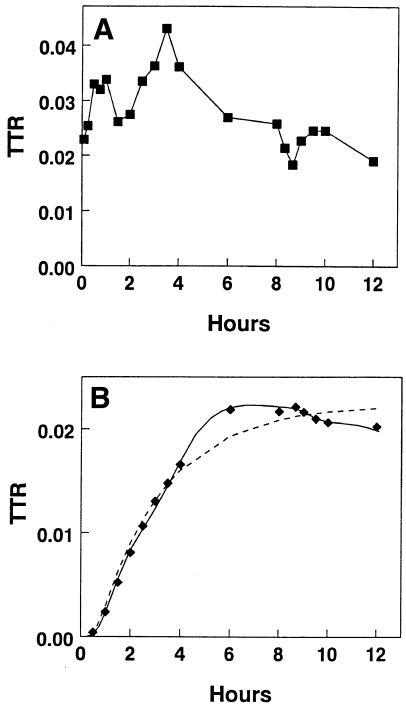

Fig. 7. Plasma palmitate and VLDL-TG palmitate TTR during a 12-h infusion of palmitate tracer in a representative subject. A: Plasma palmitate enrichment during a long-term constant infusion of $^2H_2$-palmitate. B: VLDL-TG palmitate enrichment. Dashed line, best-fitting line that describes the data as a rise-to-plateau. Solid line, VLDL-TG kinetics analyzed by the compartmental model of Fig. 1, except that the "slow" production pathway has been eliminated because it cannot be resolved using a constant infusion of tracer.

tracer, the model-derived FCR was systematically higher than the monoexponential slope over the entire range of turnover rates (Fig. 6B).

Constant infusion of palmitate tracer

During a 12-h constant infusion of labeled palmitate, plasma palmitate TTR oscillated around a quasi-steady state, but gradually drifted downward in most studies because of increasing lipolytic activity associated with continued fasting (31) (**Fig. 7A**). After a 30-min delay, VLDL-TG palmitate TTR rose steadily toward a plateau (Fig. 7B). In studies in which the plasma palmitate TTR decreased, the VLDL-TG palmitate TTR tended to decrease after reaching a peak (at 6–8 h in the subject shown in Fig. 7).

The fractional turnover rate of VLDL-TG was estimated by determining the FSR (dividing the rate of rise in TTR by the plateau TTR), or by a monoexponential rise-to-plateau mathematical model (Fig. 7B). The monoexponential rise-to-plateau model provided a higher estimate for VLDL-TG turnover than the FSR (regression line: rise-to-plateau model = 1.46 × FSR − 0.06, R^2 = 0.70; not shown). More importantly, however, both the FSR values and monoexponential rise-to-plateau model substantially underestimated, and were correlated poorly with, fractional turnover rates determined by using compartmental modeling of data generated by a simultaneous bolus of [$^2H_5$]glycerol (**Fig. 8**; regressions had non-zero intercepts, slopes = 0.13 and 0.18, and R^2 = 0.56 and 0.36, respectively).

The compartmental model shown in Fig. 1 provided an excellent description of VLDL-TG palmitate tracer kinetics obtained by constant infusion of labeled palmitate in all studies, including those in which the VLDL-TG TTR decreased after reaching a peak (Fig. 7B). In contrast to the compartmental modeling of data when the palmitate tracer was given as a bolus, constant tracer infusion did not provide sufficient shape information in the VLDL-TG TTR time course to resolve the non-systemic tracer recycling pathway from VLDL-TG turnover. It was not possible to determine whether VLDL turnover or non-systemic recycling was rate-limiting, and excellent fits to the data were achieved when the "slow" production pathway was omitted from the compartmental model. Because non-systemic tracer recycling could not be resolved, the compartmental model-derived FCR significantly underestimated, and was poorly correlated with, the turnover rate determined by using compartmental modeling of the data from a bolus of [$^2H_5$]glycerol (Fig. 8C; slope = 0.19, a non-zero intercept, and R^2 = 0.49).

DISCUSSION

In this report, we validate a new approach for measuring VLDL-TG turnover kinetics that involved the use of stable isotopically labeled glycerol or palmitate tracers, in conjunction with mathematical modeling. When the tracers

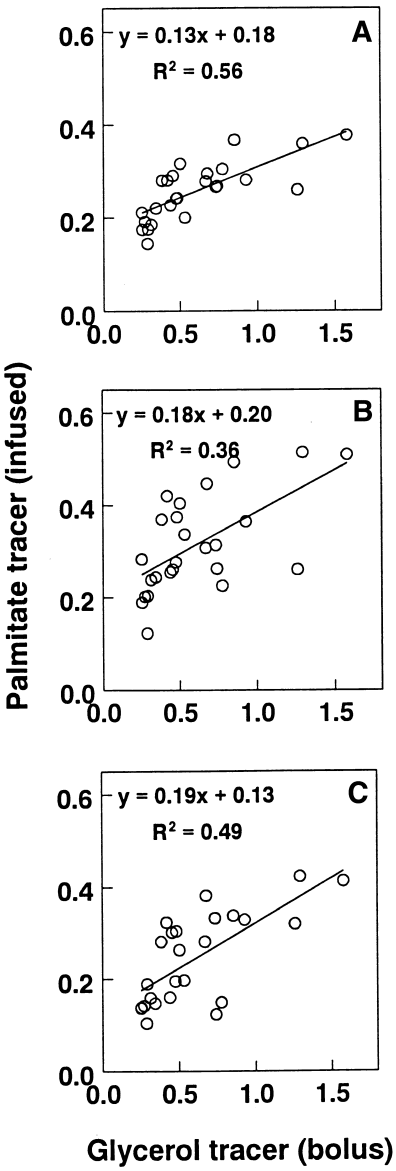

Fig. 8. Comparison of VLDL-TG turnover rates using a constant infusion of labeled palmitate and a bolus of [$^2H_5$]glycerol simultaneously. Rate constants (pools/h) for VLDL-TG turnover were measured with palmitate and glycerol tracers administered simultaneously. Abscissa = VLDL-TG fractional catabolic rate determined with bolus [$^2H_5$]glycerol and the compartmental model of Fig. 1. A: VLDL-TG fractional synthetic rate calculated from palmitate data by slope ÷ plateau. B: VLDL-TG turnover rate calculated from palmitate data by monoexponential rise-to-plateau mathematical model. C: VLDL-TG FCR determined by the compartmental model, which is able to account for non-systemic recycling of the glycerol tracer but not for the infused palmitate tracer.

were given as a bolus and the VLDL-TG turnover rate was determined by a compartmental model that was able to resolve VLDL-TG turnover kinetics apart from systemic and non-systemic tracer recycling, the glycerol and palmitate tracers provided identical values for VLDL-TG turnover rate. In contrast, when tracers were given as a bolus and VLDL-TG turnover rate was determined by the monoexponential slope technique, the palmitate tracer consistently underestimated VLDL-TG turnover rate by ~17% compared with the glycerol tracer. Moreover, the monoexponential slope attained with either glycerol or palmitate tracers was substantially slower than the VLDL-TG turnover rate derived by the compartmental model, particularly when the apparent turnover rate was >0.5 h^{-1}. In addition, when the palmitate tracer was given as a constant infusion rather than a bolus and VLDL-TG turnover rate was determined by FSR (slope ÷ plateau) analysis, the rise-to-plateau mathematical model, or by compartmental modeling, the value for VLDL-TG turnover was much lower than that obtained simultaneously by compartmental modeling of a glycerol bolus. The results from the present study cross-validate the use of a bolus injection of labeled glycerol or palmitate in conjunction with compartmental modeling to determine plasma VLDL-TG kinetics, and suggest that other methods for measuring VLDL-TG metabolism may not be reliable. It should be noted that a single compartment was adequate to describe VLDL-TG metabolism in our normolipidemic subjects. Additional compartments reflecting VLDL-TG heterogeneity may be necessary in hyperlipidemic subjects, particularly if an especially slow VLDL compartment is required to describe VLDL apolipoprotein B kinetics.

The confounding effects of tracer recycling have been recognized since the earliest studies of VLDL-TG tracer kinetics (4, 5, 32, 33). Our approach reliably resolves both systemic and non-systemic tracer recycling. Systemic tracer recycling, which is the exchange of plasma glycerol or palmitate with one or more non-plasma compartments (e.g., tissues, interstitial space), is accounted for by incorporating the plasma glycerol or palmitate time course in the compartmental model. Due to technical challenges in measuring plasma glycerol specific radioactivity, studies that involve a bolus [^{3}H]glycerol tracer with compartmental modeling usually use population-averaged rate constants, rather than measured rate constants, to describe the kinetics of the plasma glycerol subsystem (8). Moreover, these glycerol subsystem kinetics are based on [^{14}C]glycerol (34), even though [^{14}C]glycerol recycles to a greater extent than [^{3}H]glycerol (8). Stable isotopes offer an advantage over radiotracers because GC-MS provides simultaneous measurement of the numerator and denominator terms that compose the TTR, whereas assessment of specific radioactivity requires separate radioactivity and mass determinations. Therefore, our approach may provide better resolution of systemic tracer recycling because the actual time course of plasma glycerol tracer is determined for each subject.

Non-systemic tracer recycling is responsible for the "slow" synthetic pathway for VLDL-TG formation, and represents tracer that is removed from plasma, put into another pool, and later released into VLDL-TG without reappearing in plasma (8, 9, 11). This recycling compartment contains splanchnic glycerolipid pools (predominantly hepatic TG and phospholipids) and any other tracer recycling that does not involve systemic recycling of intact glycerol or palmitate, such as tracer recycling from glucose (see below). The ability of the model to resolve

non-systemic recycling from VLDL-TG turnover depends on three factors. First, the contribution of the recycling pathway can only be resolved when the turnover of the hepatic lipid pool is rate limiting (i.e., VLDL-TG turns over faster than hepatic storage lipid pools) (35). The recycling component was not always apparent when the VLDL-TG FCR was $<0.5\ h^{-1}$ for the glycerol bolus tracer. It is likely that the model based on bolus glycerol tracer kinetics may underestimate the "true" FCR at slower turnover rates ($<0.5\ h^{-1}$). Second, the contribution from recycling must be large enough to be resolved. The greater recycling of palmitate than glycerol (4) may explain why corrections for recycling were apparent for bolus palmitate tracer over the entire range of FCR, but was only apparent for bolus glycerol tracer at faster turnover rates (Fig. 6). Third, tracer must be delivered to the liver as a bolus rather than as a constant infusion, at least for the palmitate tracer. During a constant infusion of labeled palmitate, the recycling pathway dominated over the direct pathway to such an extent that the two pathways could not be resolved. The apparent VLDL-TG turnover rate measured by using an infusion of palmitate is markedly influenced by hepatic lipid turnover (non-systemic recycling), which limits the reliability of this experimental approach to measure VLDL-TG turnover.

The results of the present study underscore the importance of tracer and model selection in determining VLDL-TG kinetics. **Table 1** provides a summary of values reported for VLDL-TG turnover rate obtained during similar experimental conditions (postabsorptive state in normolipidemic subjects) using different tracers, modes of administration, and kinetic analyses. This table demonstrates that similar techniques provide similar values for VLDL-TG turnover rate, but there is marked variability in values across methods. Notably, our values for VLDL-TG turnover rate derived by bolus injection of tracer and compartmental modeling were higher than those reported using a bolus of [2-^{3}H]glycerol or constant infusion techniques.

The reason why our method, which involves a bolus of [$^2H_5$]glycerol, provides a higher value for VLDL-TG turnover than does a bolus of [^{3}H]glycerol is not known. It is possible that the presence of five deuteriums on glycerol affects the interactions among VLDL-TG, apolipoprotein C-II, and lipoprotein lipase and, thereby, alters VLDL-TG metabolism. However, this is unlikely because the values for VLDL-TG turnover obtained by using [$^2H_5$]glycerol was the same as those obtained by using [$^{13}C_1$]- or [$^2H_2$]palmitate tracers, which should not exhibit as profound an isotope effect. Moreover, we have found that values for VLDL-TG turnover obtained by using a bolus of [2-^{13}C]glycerol were

TABLE 1. Values for postabsorptive VLDL-TG fractional turnover rate determined by using different tracers and kinetic analyses

Experimental Method	VLDL-TG Turnover Rate	Number of Subjects	First Author (Reference)
	Pools/h		
Bolus injection of tracer			
Monoexponential slope			
[^{3}H]glycerol	0.22 ± 0.06	6	Sane and Nikkilä (7)
[^{3}H]glycerol	0.25 ± 0.02	34	Nikkilä and Kekki (6)
[^{3}H]glycerol	0.32 ± 0.03	6	Lemieux et al. (20)
[^{13}C]palmitate	0.47 ± 0.08	7	Present study
[$^2H_5$]glycerol	0.64 ± 0.04	16	Present study
Compartmental modeling			
[^{3}H]glycerol	0.19 ± 0.01	13	Zech et al. (8)
[^{3}H]glycerol	0.20 ± 0.03	6	Melish et al. (9)
[^{3}H]glycerol	0.33 ± 0.03	6	Lemieux et al. (20)
[^{3}H]glycerol	0.34 ± 0.11	3	Harris et al. (10)
[^{14}C]palmitate	1.02 ± 1.08	2	Quarfordt et al. (12)
[^{13}C]- or [$^2H_2$]palmitate	0.92 ± 0.24	7	Present study
[$^2H_5$]glycerol	1.06 ± 0.13	16	Present study
Constant infusion of tracer			
Rise-to-plateau			
[^{13}C]glycerol	0.28 ± 0.04	4	Siler et al. (21)
[^{13}C]palmitate	0.44 ± 0.04	6	Parks et al. (22)
[^{13}C]palmitate	0.49 ± 0.12	5	Wang et al. (23)
[^{13}C]glycerol	0.53 ± 0.12	5	Wang et al. (23)
[^{13}C]palmitate	0.43 ± 0.05	5	Present study
Acetate infusion			
$^{13}C_2$-acetate	0.38 ± 0.07	5	Aarsland et al. (43)
Isotopic dilution of labeled VLDL-TG			
[^{13}C]glycerol VLDL-TG	1.9[a]	5	Sidossis et al. (25)
Non-tracer: arteriovenous balance			
(splanchnic VLDL-TG production)	0.85 ± 0.24	7	Havel et al. (33)
	1.6 ± 0.4	19	Boberg et al. (41)

Values are mean ± SEM. Data were extracted from the indicated publications for healthy lean subjects who were studied during basal conditions and had plasma triglyceride concentration <150 mg/dl.

[a] Calculated by dividing the population-averaged production rate by the population-averaged VLDL-TG pool size, assuming a volume of distribution of 0.039 l kg^{-1}. SEM not available.

also the same as when bolus palmitate tracers were used (data not shown).

It is likely that [^{3}H]glycerol underestimates the turnover rate of VLDL-TG because of recycling of the ^{3}H apart from recycling of intact [^{3}H]glycerol from glycerolipid pools. During hepatic gluconeogenesis from glycerol, [2-^{3}H]glycerol 3-phosphate is oxidized by cytosolic NAD$^+$-linked glycerol-3-phosphate dehydrogenase to form dihydroxyacetone phosphate and NAD[^{3}H] (36), which in turn labels C-4 and C-6 of glucose (37). During hepatic glycerol oxidation, [2-^{3}H]glycerol 3-phosphate is oxidized by mitochondrial glycerol-3-phosphate oxidase, which generates H^{3}HO (38) that can label all C positions of glucose, particularly C-2, C-5, and C-6 (39, 40). These labeled glucose molecules can be used to form labeled glycerol during hepatic VLDL-TG synthesis. Recycling can also occur when label from H^{3}HO is incorporated into fatty acids during de novo lipogenesis and specific radioactivity is measured in the intact TG molecule. More than 90% of plasma glycerol is directed toward gluconeogenesis or oxidation (34) with concomitant loss of H from C-2; thus, almost all of the ^{3}H label from a [2-^{3}H]glycerol bolus is available for potential recycling into the glycerol or fatty acid moieties of VLDL-TG and contribute to an underestimation of true VLDL-TG turnover. Furthermore, peak VLDL-TG specific radioactivity appears rounded after a [2-^{3}H]glycerol bolus, so that a multi-compartment VLDL subsystem is required to describe the peak shape (8). In contrast, a single VLDL compartment is sufficient to describe the VLDL-TG peak shape in our studies that used a bolus of stable isotopically labeled glycerol or palmitate tracer and in studies that used a bolus of [^{14}C]palmitate (12) (Table 1). The blunted VLDL-TG peak shape that occurs with bolus [2-^{3}H]glycerol may result from non-systemic recycling pathways that are unique to the ^{3}H tracer, and suggests that compartmental modeling cannot adequately resolve extensive non-systemic recycling. This phenomenon may contribute to the slower values for VLDL-TG FCR observed with bolus [2-^{3}H]glycerol.

Model-independent methods of VLDL-TG turnover also support the notion that [2-^{3}H]glycerol underestimates the true VLDL-TG turnover rate. Splanchnic VLDL-TG production rates have been directly determined in human subjects by arteriovenous balance (33, 41) and by isotopic dilution of pre-labeled VLDL-TG (25). By dividing the production rate by the VLDL-TG pool size (plasma VLDL-TG concentration $\times$ plasma volume), apparent VLDL-TG turnover rates between 0.85 and 1.9 h^{-1} were obtained with these methods (Table 1). Although these approaches are technically challenging, the results suggest the "true" turnover rate of VLDL-TG may be 3- to 5-fold higher than is observed by using [^{3}H]glycerol tracer injection. The values obtained by using pre-labeled VLDL-TG were also higher than those obtained by using our approach, suggesting that our method may underestimate VLDL-TG turnover, though to a lesser degree than other tracer infusion or bolus methods. Additional studies are needed to directly compare the values for VLDL-TG turnover determined by our method with those obtained by the pre-labeled VLDL-TG infusion method.

The data from the present study demonstrate that a considerable amount of glycerol in VLDL-TG is derived from glycolytic cycling that resulted in the formation of partially de-deuterated glycerol (Fig. 3) down to the level of pyruvate (m+2) and oxaloacetate (m+1). This phenomenon was also observed by Previs et al. (42) when rat livers were perfused with [$^2H_5$]glycerol. However, this extensive carbon skeleton recycling through glycolysis and gluconeogenesis does not affect our determination of VLDL-TG turnover rate because our GC-MS method was specific for m+5 labeled glycerol. In fact, our approach remains valid even if ^{2}H lost during conversion to dihydroxyacetone phosphate is reincorporated into glycerol during gluconeogenesis, because it is unlikely that all five hydrogens on glycerol would be replaced by deuterium. Therefore, the specificity of GC-MS assures that the only non-systemic tracer recycling that affects the appearance of [$^2H_5$]glycerol in VLDL-TG involves recycling of intact glycerol, predominantly through hepatic glycerolipid pools. In contrast, a scintillation counter used for radiotracers cannot discriminate between recycled ^{3}H and recycled [2-^{3}H]glycerol. This glycolytic recycling of de-deuterated glycerol requires that the GC-MS method used to measure glycerol enrichment examine an intact molecular ion or a fragment that retains all five deuterium positions.

The precision of the GC-MS isotope ratio measurements is significantly reduced when multiple glycerol isotopomers are monitored since glycerol elutes as a very sharp peak from the chromatographic column with a peak width of about 1 s (data not shown). We therefore do not advocate routine monitoring of all glycerol isotopomers, and base the TG kinetic analysis solely on the enrichment of the m+5 isotopomer. Since the kinetics of all de-deuterated tracers were parallel on a log plot, it is apparent that metabolic transformations through glycolytic-gluconeogenic cycling occur prior to recruitment of glycerol for VLDL-TG or hepatic lipid synthesis, and inclusion of these additional isotopomers in a more comprehensive compartmental model would not help resolve VLDL-TG kinetics or tracer recycling through intrahepatic lipid stores.

In conclusion, the results of the present study demonstrate that a bolus injection of stable isotopically labeled glycerol or palmitate tracers, in conjunction with compartmental modeling, is a reliable approach for measuring VLDL-TG turnover rate. Values for VLDL-TG turnover rate obtained with compartmental modeling are faster than those obtained using a monoexponential slope analysis, and values obtained with bolus stable isotopically labeled glycerol and palmitate are faster than those obtained using a constant infusion protocol or a bolus of [2-^{3}H]glycerol. The differences in results observed between methods are likely due to differences in their ability to resolve hepatic glycerolipid tracer recycling, which can only be resolved by using the appropriate tracer and mathematical model. The use of [$^2H_5$]glycerol has several advantages over the use of other tracers because of less recycling and greater ease in measuring very low isotopic enrichments generated during the descending tail of the

curve, when resolution of the recycling pathway is particularly important.

This work was supported by NIH grants DK37948, CA62177, DK56341 (Clinical Nutrition Research Unit), RR-00036 (General Clinical Research Center), and RR-00954 (Biomedical Mass Spectrometry Resource).

Manuscript received 11 July 2001 and in revised form 22 October 2001.

REFERENCES

1. Reaven, G. M., Y. D. I. Chen, J. Jeppesen, P. Maheux, and R. M. Krauss. 1993. Insulin resistance and hyperinsulinemia in individuals with small, dense, low density lipoprotein particles. *J. Clin. Invest.* **92:** 141–146.
2. Brown, C. D., M. Higgins, K. A. Donato, F. C. Rohde, R. Garrison, E. Obarzanek, N. D. Ernst, and M. Horan. 2000. Body mass index and the prevalence of hypertension and dyslipidemia. *Obes. Res.* **8:** 605–619.
3. Assmann, G., and H. Schulte. 1992. Relation of high-density lipoprotein cholesterol and triglycerides to incidence of atherosclerotic coronary artery disease (the PROCAM Experience). *Am. J. Cardiol.* **70:** 733–737.
4. Farquhar, J. W., R. C. Gross, R. M. Wagner, and G. M. Reaven. 1965. Validation of an incompletely coupled two-compartment nonrecycling catenary model for turnover of liver and plasma triglyceride in man. *J. Lipid Res.* **6:** 119–134.
5. Reaven, G. M., D. B. Hill, R. C. Gross, and J. W. Farquhar. 1965. Kinetics of triglyceride turnover of very low density lipoproteins of human plasma. *J. Clin. Invest.* **44:** 1826–1833.
6. Nikkilä, E. A., and M. Kekki. 1971. Polymorphism of plasma triglyceride kinetics in normal human adult subjects. *Acta Med. Scand.* **190:** 49–59.
7. Sane, T., and E. A. Nikkilä. 1988. Very low density lipoprotein triglyceride metabolism in relatives of hypertriglyceridemic probands. Evidence for genetic control of triglyceride removal. *Arterioscler.* **8:** 217–226.
8. Zech, L. A., S. M. Grundy, D. Steinberg, and M. Berman. 1979. Kinetic model for production and metabolism of very low density lipoprotein triglycerides. Evidence for a slow production pathway and results for normolipidemic subjects. *J. Clin. Invest.* **63:** 1262–1273.
9. Melish, J., N. A. Le, H. Ginsberg, D. Steinberg, and W. V. Brown. 1980. Dissociation of apoprotein B and triglyceride production in very- low-density lipoproteins. *Am. J. Physiol.* **239:** E354–E362.
10. Harris, W. S., W. E. Connor, R. D. Illingworth, D. W. Rothrock, and D. M. Foster. 1990. Effects of fish oil on VLDL triglyceride kinetics in humans. *J. Lipid Res.* **31:** 1549–1558.
11. Barrett, P. H., N. Baker, and P. J. Nestel. 1991. Model development to describe the heterogeneous kinetics of apolipoprotein B and triglyceride in hypertriglyceridemic subjects. *J. Lipid Res.* **32:** 743–762.
12. Quarfordt, S. H., A. Frank, D. M. Shames, M. Berman, and D. Steinberg. 1970. Very low density lipoprotein triglyceride transport in type IV hyperlipoproteinemia and the effects of carbohydrate-rich diets. *J. Clin. Invest.* **49:** 2281–2297.
13. Lichtenstein, A. H., J. S. Cohn, D. L. Hachey, J. S. Millar, J. M. Ordovas, and E. J. Schaefer. 1990. Comparison of deuterated leucine, valine, and lysine in the measurement of human apolipoprotein A-I and B-100 kinetics. *J. Lipid Res.* **31:** 1693–1701.
14. Patterson, B. W., D. L. Hachey, G. L. Cook, J. M. Amann, and P. D. Klein. 1991. Incorporation of a stable isotopically labeled amino acid into multiple human apolipoproteins. *J. Lipid Res.* **32:** 1063–1072.
15. Parhofer, K. G., P. H. R. Barrett, D. M. Bier, and G. Schonfeld. 1991. Determination of kinetic parameters of apolipoprotein B metabolism using amino acids labeled with stable isotopes. *J. Lipid Res.* **32:** 1311–1323.
16. Reeds, P. J., D. L. Hachey, B. W. Patterson, K. J. Motil, and P. D. Klein. 1992. VLDL apolipoprotein B-100, a potential indicator of the isotopic labeling of the hepatic protein synthetic precursor pool in humans: studies with multiple stable isotopically labeled amino acids. *J. Nutr.* **122:** 457–466.
17. Demant, T., C. J. Packard, H. Demmelmair, P. Stewart, A. Bedynek, D. Bedford, D. Seidel, and J. Shepherd. 1996. Sensitive methods to study human apolipoprotein B metabolism using stable isotope-labeled amino acids. *Am. J. Physiol.* **270:** E1022–E1036.
18. Elias, N., B. W. Patterson, and G. Schonfeld. 1999. Decreased production rates of VLDL triglycerides and apoB-100 in subjects heterozygous for familial hypobetalipoproteinemia. *Arterioscler. Thromb. Vasc. Biol.* **19:** 2714–2721.
19. Elias, N., B. W. Patterson, and G. Schonfeld. 2000. In vivo metabolism of apoB, apoA-I and VLDL triglycerides in a form of hypobetalipoproteinemia not linked to the apoB gene. *Arterioscler. Thromb. Vasc. Biol.* **20:** 1309–1315.
20. Lemieux, S., B. W. Patterson, A. Carpentier, G. F. Lewis, and G. Steiner. 1999. A stable isotope method using a [$^2H_5$]glycerol bolus to measure very low density lipoprotein triglyceride kinetics in humans. *J. Lipid Res.* **40:** 2111–2117.
21. Siler, S. Q., R. A. Neese, E. J. Parks, and M. K. Hellerstein. 1998. VLDL-triglyceride production after alcohol ingestion, studied using [2-$^{13}C_1$]glycerol. *J. Lipid Res.* **39:** 2319–2328.
22. Parks, E. J., R. M. Krauss, M. P. Christiansen, R. A. Neese, and M. K. Hellerstein. 1999. Effects of a low-fat, high-carbohydrate diet on VLDL-triglyceride assembly, production, and clearance. *J. Clin. Invest.* **104:** 1087–1096.
23. Wang, W., A. Basinger, R. A. Neese, B. Shane, S. A. Myong, M. Christiansen, and M. K. Hellerstein. 2001. Effect of nicotinic acid administration on hepatic very low density lipoprotein-triglyceride production. *Amer. J. Physiol. Endocrinol. Met.* **43**:E540–E547.
24. Hellerstein, M. K., M. Christiansen, S. Kaempfer, C. Kletke, K. Wu, J. S. Reid, K. Mulligan, N. S. Hellerstein, and C. H. L. Shackleton. 1991. Measurement of de novo hepatic lipogenesis in humans using stable isotopes. *J. Clin. Invest.* **87:** 1841–1852.
25. Sidossis, L., B. Mittendorfer, E. Walser, D. Chinkes, and R. R. Wolfe. 1998. Hyperglycemia-induced inhibition of splanchnic fatty acid oxidation increases hepatic triacylglycerol secretion. *Am. J. Physiol.* **275:** E798–E805.
26. Klein, R. L., and D. B. Zilversmit. 1984. Direct determination of human and rabbit apolipoprotein B selectively precipitated with butanol-isopropyl ether. *J. Lipid Res.* **25:** 1380–1386.
27. Patterson, B. W., G. Zhao, N. Elias, D. L. Hachey, and S. Klein. 1999. Validation of a new procedure to determine plasma fatty acid concentration and isotopic enrichment. *J. Lipid Res.* **40:** 2118–2124.
28. Patterson, B. W., and R. R. Wolfe. 1993. Concentration dependence of methyl palmitate isotope ratios by electron impact ionization gas chromatography/mass spectrometry. *Biol. Mass Spectrom.* **22:** 481–486.
29. Gilker, C. D., G. R. Pesola, and D. E. Matthews. 1992. A mass spectrometric method for measuring glycerol levels and enrichments in plasma using ^{13}C and ^2H stable isotopic tracers. *Anal. Biochem.* **205:** 172–178.
30. Patterson, B. W. 1997. Use of stable isotopically labeled tracers for studies of metabolic kinetics: an overview. *Metabolism.* **46:** 322–329.
31. Klein, S., Y. Sakurai, J. A. Romijn, and R. M. Carroll. 1993. Progressive alterations in lipid and glucose metabolism during short-term fasting in young adult men. *Am. J. Physiol.* **265:** E801–E806.
32. Havel, R. J. 1961. Conversion of plasma free fatty acids into triglycerides of plasma lipoprotein fractions in man. *Metab. Clin. Exp.* **10:** 1031–1034.
33. Havel, R. J., J. P. Kane, E. O. Balasse, N. Segel, and L. V. Basso. 1970. Splanchnic metabolism of free fatty acids and production of triglycerides of very low density lipoproteins in normotriglyceridemic and hypertriglyceridemic humans. *J. Clin. Invest.* **49:** 2017–2035.
34. Malmendier, C. L., C. Delcroix, and M. Berman. 1974. Interrelations in the oxidative metabolism of free fatty acids, glucose, and glycerol in normal and hyperlipemic patients. A compartmental model. *J. Clin. Invest.* **54:** 461–476.
35. Gross, R. C., E. H. Eigenbrodt, and J. W. Farquhar. 1967. Endogenous triglyceride turnover in liver and plasma of the dog. *J. Lipid Res.* **8:** 114–125.
36. Rognstad, R., and D. G. Clark. 1974. Tritium as a tracer for reducing equivalents in isolated liver cells. *Eur. J. Biochem.* **42:** 51–60.
37. Hoberman, H. D., and A. F. D'Adamo. 1960. Coupling of oxida-

tion of substrates to reductive biosyntheses. IV. Studies with 2,2′-D-fumarate and 2,2'-C^{14}-fumarate. *J. Biol. Chem.* **235:** 519–522.
38. Rognstad, R. 1991. Estimation of peroxisomal and mitochondrial fatty acid oxidation in rat hepatocytes using tritiated substrates. *Biochem. J.* **279:** 147–150.
39. Postle, A. D., and D. P. Bloxham. 1980. The use of tritiated water to measure absolute rates of hepatic glycogen synthesis. *Biochem. J.* **192:** 65–73.
40. Landau, B. R., J. Wahren, V. Chandramouli, W. C. Schumann, K. Ekberg, and S. Kalhan. 1996. Contributions of gluconeogenesis to glucose production in the fasted state. *J. Clin. Invest.* **98:** 378–385.
41. Boberg, J., L. A. Carlson, U. Freyschuss, B. W. Lassers, and M. L. Wahlqvist. 1972. Splanchnic secretion rates of plasma triglycerides and total and splanchnic turnover of plasma free fatty acids in men with normo- and hypertriglyceridaemia. *Eur. J. Clin. Invest.* **2:** 454–466.
42. Previs, S. F., C. A. Fernandez, D. Yang, M. V. Soloviev, F. David, and H. Brunengraber. 1995. Limitations of the mass isotopomer distribution analysis of glucose to study gluconeogenesis. Substrate cycling between glycerol and triose phosphates in liver. *J. Biol. Chem.* **270:** 19806–19815.
43. Aarsland, A., D. Chinkes, and R. R. Wolfe. 1996. Contributions of de novo synthesis of fatty acids to total VLDL-triglyceride secretion during prolonged hyperglycemia/hyperinsulinemia in normal man. *J. Clin. Invest.* **98:** 2008–2017.